

Crystal Structure of *Thermotoga maritima* Ribosome Recycling Factor: A tRNA Mimic

Maria Selmer,¹ Salam Al-Karadaghi,¹ Go Hirokawa,² Akira Kaji,² Anders Liljas^{1*}

Ribosome recycling factor (RRF), together with elongation factor G (EF-G), catalyzes recycling of ribosomes after one round of protein synthesis. The crystal structure of RRF was determined at 2.55 angstrom resolution. The protein has an unusual fold where domain I is a long three-helix bundle and domain II is a three-layer $\beta/\alpha/\beta$ sandwich. The molecule superimposes almost perfectly with a transfer RNA (tRNA) except that the amino acid-binding 3' end is missing. The mimicry suggests that RRF interacts with the posttermination ribosomal complex in a similar manner to a tRNA, leading to disassembly of the complex. The structural arrangement of this mimicry is entirely different from that of other cases of less pronounced mimicry of tRNA so far described.

Protein synthesis, one of life's fundamental processes, usually is divided into three steps: initiation, elongation, and termination. However, there is a fourth essential step, ribosome recycling or disassembly of the posttermination complex. In bacteria, this is catalyzed by RRF (1–3).

During the termination step, stop codons are recognized by release factors RF1 or RF2 (4), leading to peptidyl-tRNA hydrolysis and peptide release. These factors are then released from the ribosome by RF3 (5, 6). The resulting posttermination complex presumably consists of a 70S ribosome with a bound mRNA, an empty A-site, and a deacylated tRNA in the P-site. RRF and elongation factor G (EF-G) under guanosine triphosphate (GTP) hydrolysis disassemble this posttermination complex (7, 8).

RRF is an essential protein for prokaryotes (9). In the absence of RRF, the ribosome remains bound to the mRNA and initiates unscheduled translation downstream from the termination codon (10) without initiation signals. Here we present the crystal structure of RRF and suggest a functional hypothesis based on the structure.

The crystal structure of *Thermotoga maritima* RRF was determined at 2.55 Å resolution by multiwavelength anomalous dispersion (MAD) (11) (Table 1). A portion of the experimental map at 2.9 Å resolution is shown in Fig. 1A.

Thermotoga maritima RRF has overall dimensions of 70 Å by 47 Å by 20 Å and

consists of two domains (Fig. 1B). Domain I is a three-helix bundle containing residues 2 to 30 and 105 to 185. Helices H1, H5, and H6 are tightly packed against each other with an unusual slightly right-handed twist. The angles between the helices are 9°, 9°, and 13°, respectively. The helices H1 and H6 are straight, whereas helix H5 is slightly bent. About one-third of the residues in its hydrophobic core are isoleucins (Fig. 2).

Domain II is a three-layer $\beta/\alpha/\beta$ sandwich inserted into domain I and consists of residues 31 to 104. A two-stranded antiparallel β ribbon and a four-stranded antiparallel β sheet are positioned on the top and bottom of the three helices. Two of the helices, H2 and H3, are short 3_{10} -helices.

For domain I, the programs DALI (12) and TOP (13) failed to find any significant matches. Other three-helix bundles are gen-

erally less tightly packed and are arranged as left-handed supercoils. For domain II the closest match is the NH₂-terminal domain of a thermostable B DNA polymerase (Protein Data Bank code 1tgo) (14) that lacks H3 and $\beta 6$. For 64 aligned amino acids the root-mean-square (rms) deviation is 2.7 Å.

RRF is present in all organisms whose genomes have been sequenced (15) except for Archaea (16) and is generally well conserved in terms of residue identity and length (Fig. 2). The conserved residues are mapped on the ribbon structure in Fig. 1B. Most of the exposed conserved residues are basic and are located in or near helix 5. Domain I has also a prominent cluster of negative charges, primarily on one side owing to sequences containing between 20 and 29 acidic residues in this domain. The water-accessible surface area lost in the domain-domain interaction is 981 Å² (8.2%) out of the domain areas (GRASP) (17). This is lower than normal (18) and may indicate a weak interaction between the domains. In addition, the proportion of charged amino acid residues at this interface, 11 out of 26 (42%), is higher than normal (18).

Superposition of *T. maritima* RRF and yeast tRNA^{Phe} (19) reveals a marked similarity (Fig. 3, A and C). The dimensions of the molecules are closely identical if one disregards the CCA end, where the amino acid is attached to tRNA. The width of RRF is only slightly bigger in the acceptor stem part, whereas the tRNA has a slightly more pronounced elbow. The absence of conserved residues in the region corresponding to the anticodon loop of tRNA (Fig. 1B) indicates that this region of RRF is not involved in specific interactions. The marked similarity of RRF and tRNA is consistent with the suggestion that RRF binds to the ribosome in

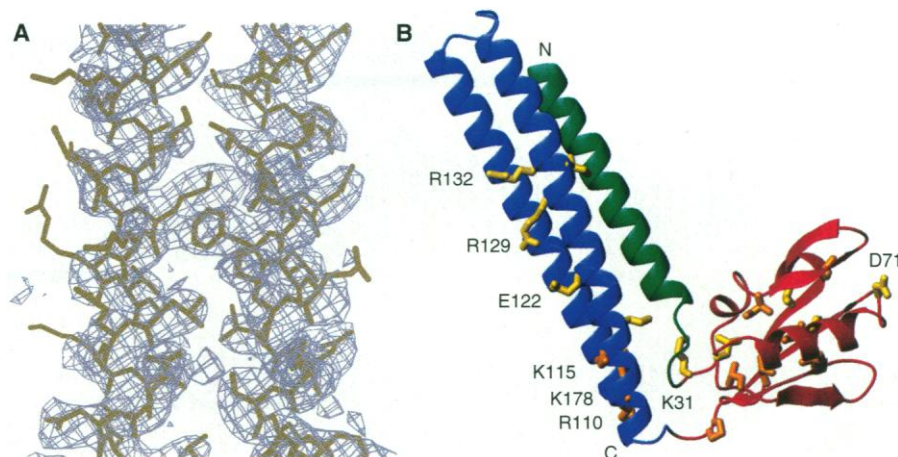


Fig. 1. (A) A portion of the 2.9 Å MAD map after DM contoured at 1.0 σ with O (34) superimposed on residue 4–24 (H1, left) and 157–176 (H6, right) of the final refined model. (B) Molmol (34) ribbon representation of RRF. The chain starts from domain I (green), then goes through domain II (red) and back to domain I (blue). The conserved and conservatively substituted amino acids are marked with orange (all known sequences) and yellow (for bacteria and chloroplast).

¹Molecular Biophysics, Center for Chemistry and Chemical Engineering, Lund University, Post Office Box 124, SE-22100 Lund, Sweden. ²Department of Microbiology, School of Medicine, University of Pennsylvania, Philadelphia, PA 19104, USA.

*To whom correspondence should be addressed. E-mail: anders.liljas@mbfys.ln.se

REPORTS

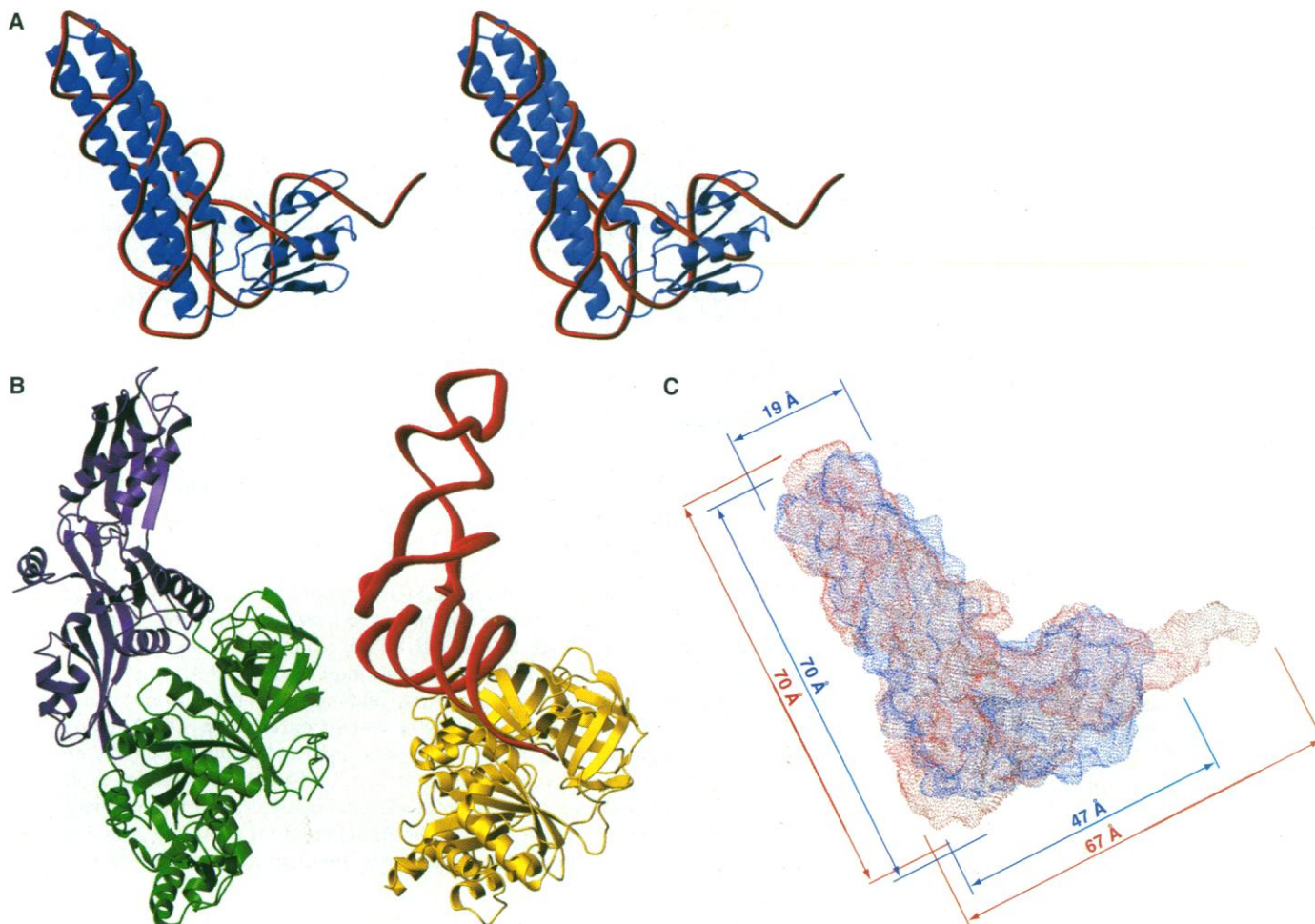


Fig. 3. (A) Stereo ribbon representation of the superposition of RRF (blue) and yeast tRNA^{Phe} (red) with Molmol (34). (B) Comparison of EF-G (36) and the ternary complex of EF-Tu + GDPNP + aatRNA (32). EF-G (left) is similar in shape to EF-Tu + GDPNP + aatRNA (right). Domain III-IV of EF-G (purple) imitates the shape of the tRNA (red) bound to EF-Tu (yellow). The remaining

domains of EF-G (green) are structurally similar to EF-Tu. RRF (A) imitates the tRNA in a totally different manner. (C) Grasp (34) surface representation of the superposition of RRF (blue) and yeast tRNA^{Phe} (red). The shapes and sizes of the surfaces are nearly identical except for the acceptor end of tRNA (to the right), which has no corresponding part in RRF.

sociate from the ribosome, resulting in the release of ribosomes from mRNA (6, 7, 25) (because there is no tRNA to stabilize its ribosome binding), followed by dissociation into subunits, especially in the presence of IF3 (1, 26). When the ribosomes have strong affinity to the mRNA due either to a proximal SD sequence (8) or to the mRNA configuration (27), RRF may not move into the P-site but may instead reach an intermediate site. The mRNA remains bound to the ribosome, and thus P-site tRNA remains bound because of the codon-anticodon interaction. Dissociation of the subunits will occur before the release of tRNA (8) under these conditions. For the release of this tRNA, IF3 is required (8, 28).

If similar binding of RRF to the A-site also can take place during elongation, this may be part of the mechanism for the reduction of translational error (2) and for the accidental release of peptidyl tRNA from the ribosomes by RRF (29).

GTP analogs, which keep EF-G bound to

the ribosomes (30), inhibit the RRF reaction (8, 25). So does the antibiotic fusidic acid, which also locks EF-G on the ribosome (21). These observations support the hypothesis that EF-G release is a prerequisite for ribosomal disassembly.

Mutations of the conserved residues Arg 110, 129, and 132 (Figs. 1B and 2) produce nonfunctional *Escherichia coli* RRF (31). In our superposition, Arg 129 and 132 partly overlap with the minor groove near positions 31 and 41 of tRNA (Fig. 3A). This part of the tRNA has no contacts in the spacious A-site, but constitutes one of the ribosome-interacting regions of tRNA in the tighter P-site (23). To allow these residues to be functionally critical, RRF has to move to the P-site where they can take part in an interaction.

RRF is not the first case of protein-tRNA mimicry. As shown in Fig. 3B, the overall shape of the three-dimensional structure of EF-G is similar to that of the ternary complex of EF-Tu, GDPNP, and aminoacyl-tRNA (32). Although domain I of RRF and domain

IV of EF-G mimic the same portion of tRNA, they have no structural similarity, indicating that there are various ways for proteins to mimic tRNA. IF1 (33) may also mimic the anticodon stem of tRNA. However, none of the cases of mimicry discussed above constitute the near perfect mimicry of tRNA as represented by RRF (Fig. 3, A to C).

References and Notes

1. L. Janosi, H. Hara, S. Zhang, A. Kaji, *Adv. Biophys.* **32**, 121 (1996).
2. L. Janosi, R. Ricker, A. Kaji, *Biochimie* **78**, 959 (1996).
3. A. Kaji, E. Teyssier, G. Hirokawa, *Biochem. Biophys. Res. Commun.* **250**, 1 (1998).
4. E. M. Scolnick, R. Tompkins, C. T. Caskey, M. Nirenberg, *Proc. Natl. Acad. Sci. U.S.A.* **61**, 768 (1968).
5. D. V. Freistroffer, M. Y. Pavlov, J. MacDougall, R. H. Buckingham, M. Ehrenberg, *EMBO J.* **16**, 4126 (1997).
6. G. Grentzmann et al., *RNA* **4**, 973 (1998).
7. A. Hirashima and A. Kaji, *J. Mol. Biol.* **65**, 43 (1972).
8. R. Karimi, M. Pavlov, R. Buckingham, M. Ehrenberg, *Mol. Cell* **3**, 601 (1999).
9. L. Janosi, I. Shimizu, A. Kaji, *Proc. Natl. Acad. Sci. U.S.A.* **91**, 4249 (1994).
10. M. Ryoji, R. Berland, A. Kaji, *Proc. Natl. Acad. Sci. U.S.A.* **78**, 5973 (1981); L. Janosi et al., *EMBO J.* **17**, 1141 (1998).

11. Selenomethionyl RRF was purified and crystallized as described for wild-type *T. maritima* RRF [A. Kaji, in preparation; M. Selmer, S. Al-Karadaghi, G. Hirokawa, A. Kaji, A. Liljas, *Acta Crystallogr.* **D55**, 2049 (1999)] except that 5 mM dithiothreitol was used throughout purification and crystallization. Selenomethionine incorporation at all four positions was confirmed by electrospray mass spectroscopy (EMS). MAD data at the selenium edge were collected at BM14, European Synchrotron Radiation Facility (ESRF), France, on a MAR345 Image Plate detector. MAD data were processed with Mosflm [A. G. W. Leslie, *CCP4 ESF-EACMB Newslett. Protein Crystallogr.* **26** (1992)], SCALA, and TRUNCATE [CCP4, *Acta Crystallogr.* **D50**, 760 (1994)]. Three selenium sites were found with SHELXS-97 (Patterson superposition) [G. M. Sheldrick, *Methods Enzymol.* **276**, 628 (1997)] and SHELXC (dual-space methods) [G. M. Sheldrick, in *Direct Methods for Solving Macromolecular Structures*, S. Fortier, Ed. (Kluwer, Dordrecht, Netherlands, 1998), pp. 401–411] and were used to calculate phases to 4.0 Å with MLPHARE (CCP4). Solvent flattening and phase extension to 2.9 Å with DM (CCP4) improved the map and allowed tracing of 184 amino acid residues in the p4₂,2₂ map. Model building was performed with the program O [T. A. Jones, J.-Y. Zou, S. W. Cowan, M. Kjeldgaard, *Acta Crystallogr.* **A47**, 110 (1991)]. The model was refined with CNS [A. T. Brünger *et al.*, *Acta Crystallogr.* **D54**, 905 (1998)] against the 2.55 Å native data. The final model includes 184 protein residues, 2 acetate ions, and 65 water molecules. The current *R* factor and *R*_{free} (using 5% of the data) are 23.0 and 27.7%, respectively. The refined model has no residues in the disallowed region of the Ramachandran plot according to PROCHECK [R. A. Laskowski, M. V. MacArthur, D. S. Moss, J. M. Thornton, *J. Appl. Crystallogr.* **26**, 283 (1993)].
12. L. Holm and C. Sander, *J. Mol. Biol.* **233**, 123 (1993).
13. G. Lu, *PDB Q. Newslett.* **78**, 10 (1996).
14. K.-P. Hopfner *et al.*, *Proc. Natl. Acad. Sci. U.S.A.* **96**, 3600 (1999).
15. T. Kanai *et al.*, *Eur. J. Biochem.* **256**, 212 (1998); C. Ouzounis, P. Bork, G. Casari, C. Sander, *Protein Sci.* **4**, 2424 (1995); N. Rolland *et al.*, *Proc. Natl. Acad. Sci. U.S.A.* **96**, 5464 (1999).
16. J. Bult *et al.*, *Science* **273**, 1058 (1996); H. P. Klenk *et al.*, *Nature* **390**, 364 (1997).
17. A. Nicholls, K. A. Sharp, B. Honig, *Proteins* **11**, 281 (1991).
18. P. Argos, *Protein Eng.* **2**, 101 (1988).
19. A. Jack, J. E. Ladner, A. Klug, *J. Mol. Biol.* **108**, 619 (1976).
20. M. Y. Pavlov, D. V. Freistroffer, V. Heurgué-Hamard, R. H. Buckingham, M. Ehrenberg, *J. Mol. Biol.* **273**, 389 (1997).
21. A. Hirashima and A. Kaji, *J. Biol. Chem.* **248**, 7580 (1973).
22. H. Stark *et al.*, *Cell* **88**, 19 (1997); R. Agrawal *et al.*, *Science* **271**, 1000 (1996); R. Agrawal *et al.*, *J. Biol. Chem.* **274**, 8723 (1999).
23. J. H. Cate, M. M. Yusupov, G. Z. Yusupova, T. N. Earnest, H. F. Noller, *Science* **285**, 2095 (1999).
24. H. Ishitsuka, Y. Kuriki, A. Kaji, *J. Biol. Chem.* **245**, 3346 (1970).
25. K. Ogawa and A. Kaji, *Eur. J. Biochem.* **658**, 411 (1975).
26. A. R. Subramanian and B. D. Davis, *Nature* **228**, 1273 (1970).
27. Y. Inokuchi *et al.*, *J. Biochem.* **99**, 1169 (1986).
28. C. Gualerzi, C. L. Pon, A. Kaji, *Biochem. Biophys. Res. Commun.* **45**, 1312 (1971).
29. V. Heurgué-Hamard *et al.*, *EMBO J.* **17**, 808 (1998).
30. N. Inoue-Yokosawa, C. Ishikawa, Y. Kaziro, *J. Biol. Chem.* **249**, 4321 (1974).
31. L. Janosi *et al.*, *J. Mol. Biol.*, in press.
32. A. Åvarsson *et al.*, *EMBO J.* **13**, 3669 (1994); J. Czworkowski, J. Wang, T. A. Steitz, P. B. Moore, *EMBO J.* **13**, 3661 (1994); P. Nissen *et al.*, *Science* **270**, 1464 (1995).
33. M. Sette *et al.*, *EMBO J.* **16**, 1436 (1997).
34. Figures: O [T. A. Jones, J.-Y. Zou, S. W. Cowan, M. Kjeldgaard, *Acta Crystallogr.* **A47**, 110 (1991)]; Molmol [R. Koradi, M. Billeter, K. Wuthrich, *J. Mol. Graphics* **14**, 51 (1996)]; ClustalX [J. D. Thompson, T. J. Gibson, F. Plewniak, F. Jeanmougin, D. G. Higgins,

- Nucleic Acids Res.* **24**, 4876 (1997)]; Alscript [G. J. Barton, *Protein Eng.* **6**, 37 (1993)]; Grasp [A. Nicholls, K. A. Sharp, B. Honig, *Proteins* **11**, 281 (1991)].
35. Y. Zhang and L. L. Spemulli, *Biochim. Biophys. Acta* **1443**, 245 (1998).
 36. M. Laurberg, personal communication.
 37. We thank P. Lipniunas (Astra-Zeneca, Sweden) for EMS of selenomethionyl RRF, and the tutors and participants in the 3rd European Molecular Biology Organization-sponsored MAD workshop, especially G. Leonard (ESRF, France) and T. Schneider, for assistance with data col-

lection and the search for selenium positions. Native data were collected at the MAX synchrotron at experimental station 711. M.S. is the recipient of a graduate student fellowship from the Swedish Foundation for Strategic Research through SBNet. The project was supported by grants to A.L. from the Swedish Natural Science Research Council and the European Union (BIO4-CT97-2188). Coordinates of RRF and structure factor amplitudes have been deposited in the Protein Data Bank (accession code 1dd5).

2 November 1999; accepted 16 November 1999

Microglial Activation Resulting from CD40-CD40L Interaction After β -Amyloid Stimulation

Jun Tan,^{1*} Terrence Town,^{1*} Daniel Paris,^{1*} Takashi Mori,¹ Zhiming Suo,¹ Fiona Crawford,¹ Mark P. Mattson,² Richard A. Flavell,³ Michael Mullan^{1†}

Alzheimer's disease (AD) has a substantial inflammatory component, and activated microglia may play a central role in neuronal degeneration. CD40 expression was increased on cultured microglia treated with freshly solubilized amyloid- β (A β , 500 nanomolar) and on microglia from a transgenic murine model of AD (Tg APP_{sw}). Increased tumor necrosis factor α production and induction of neuronal injury occurred when A β -stimulated microglia were treated with CD40 ligand (CD40L). Microglia from Tg APP_{sw} mice deficient for CD40L demonstrated reduction in activation, suggesting that the CD40-CD40L interaction is necessary for A β -induced microglial activation. Finally, abnormal tau phosphorylation was reduced in Tg APP_{sw} animals deficient for CD40L, suggesting that the CD40-CD40L interaction is an early event in AD pathogenesis.

It has been suggested that A β activation of microglial cells may be involved in the inflammatory component of AD (1, 2). However, the mechanisms of microglial activation by A β remain speculative. As CD40, an important receptor involved in cellular signaling and activation, plays a key role in inflammation (3), we investigated whether the interaction of CD40-CD40L with A β activates microglia. We used reverse transcriptase polymerase chain reaction (RT-PCR), protein immunoblot, and flow cytometry [fluorescence-activated cell sorting (FACS)] to determine whether A β could specifically induce CD40 expression on cultured microglial cells after treatment with a low dose (500 nM) of freshly solubilized A β ₁₋₄₀ or A β ₁₋₄₂. The potentially pathogenic peptides A β ₁₋₄₀ or A β ₁₋₄₂ induced CD40 expression on cultured microglial cells when compared with A β -free, reverse A β (A β ₄₀₋₁) or the 695 iso-

form of soluble amyloid precursor protein (sAPP α -695) (4, 5) (Web fig. 1) (6). To see whether endogenous overexpression of A β could lead to microglial CD40 expression, we measured CD40 expression on microglia from a transgenic mouse model of AD (Tg APP_{sw}, overexpressing A β ₁₋₄₀ and A β ₁₋₄₂) (7) and control (wild-type) littermates (4). Microglia from Tg APP_{sw} newborn mice had markedly increased levels of soluble A β ₁₋₄₀ compared with control littermates (8), and the CD40-expressing cell fraction was markedly increased in primary cultured microglia from Tg APP_{sw} mice compared with microglia from control littermates (Web fig. 2) (6). CD40 expression was increased in microglia from control littermates exposed to A β ₁₋₄₂ and in Tg APP_{sw} microglia reexposed to exogenous A β ₁₋₄₂ compared with those exposed to A β ₄₀₋₁ or sAPP α -695 (Web fig. 2) (6). These data show that A β peptides specifically induce CD40 expression in primary cultured and N9 microglia.

To examine whether proinflammatory cytokines could regulate A β -dependent CD40 expression, we treated A β -challenged microglia with low doses of interleukin-1 β (IL-1 β), IL-2, IL-4, IL-6, IL-12, or interferon- γ (IFN- γ) (4), as the expression of CD40 has been shown to be variously regulated by these cytokines on human thymic epithelial cells, human endothelial cells, and keratinocytes (9). Only a low dose

¹The Roskamp Institute, University of South Florida, 3515 East Fletcher Avenue, Tampa, FL 33613, USA. ²Sanders-Brown Research Center on Aging and Department of Anatomy and Neurobiology, University of Kentucky, Lexington, KY 40536, USA. ³Howard Hughes Medical Institute, Yale University School of Medicine, 310 Cedar Street, New Haven, CT 06520, USA.

*These authors contributed equally to this work.
†To whom correspondence should be addressed. E-mail: mmullan@com1.med.usf.edu

LINKED CITATIONS

- Page 1 of 3 -



You have printed the following article:

Crystal Structure of *Thermotoga maritima* Ribosome Recycling Factor: A tRNA Mimic

Maria Selmer; Salam Al-Karadaghi; Go Hirokawa; Akira Kaji; Anders Liljas

Science, New Series, Vol. 286, No. 5448. (Dec. 17, 1999), pp. 2349-2352.

Stable URL:

<http://links.jstor.org/sici?sici=0036-8075%2819991217%293%3A286%3A5448%3C2349%3ACSOTMR%3E2.0.CO%3B2-M>

This article references the following linked citations:

References and Notes

⁴ **Release Factors Differing in Specificity for Terminator Codons**

E. Scolnick; R. Tompkins; T. Caskey; M. Nirenberg

Proceedings of the National Academy of Sciences of the United States of America, Vol. 61, No. 2. (Oct. 15, 1968), pp. 768-774.

Stable URL:

<http://links.jstor.org/sici?sici=0027-8424%2819681015%2961%3A2%3C768%3ARFDISF%3E2.0.CO%3B2-Y>

⁹ **Ribosome Recycling Factor (Ribosome Releasing Factor) is Essential for Bacterial Growth**

Laszlo Janosi; Ichiro Shimizu; Akira Kaji

Proceedings of the National Academy of Sciences of the United States of America, Vol. 91, No. 10. (May 10, 1994), pp. 4249-4253.

Stable URL:

<http://links.jstor.org/sici?sici=0027-8424%2819940510%2991%3A10%3C4249%3ARRF%28RF%3E2.0.CO%3B2-F>

¹⁰ **Reinitiation of Translation from the Triplet next to the Amber Termination Codon in the Absence of Ribosome-Releasing Factor**

Masaru Ryoji; Robert Berland; Akira Kaji

Proceedings of the National Academy of Sciences of the United States of America, Vol. 78, No. 10, [Part 2: Biological Sciences]. (Oct., 1981), pp. 5973-5977.

Stable URL:

<http://links.jstor.org/sici?sici=0027-8424%28198110%2978%3A10%3C5973%3AROTFTT%3E2.0.CO%3B2-3>

NOTE: The reference numbering from the original has been maintained in this citation list.

LINKED CITATIONS

- Page 2 of 3 -



¹⁴ **Crystal Structure of a Thermostable Type B DNA Polymerase from *Thermococcus gorgonarius***

Karl-Peter Hopfner; Andreas Eichinger; Richard A. Engh; Frank Laue; Waltraud Ankenbauer; Robert Huber; Bernhard Angerer

Proceedings of the National Academy of Sciences of the United States of America, Vol. 96, No. 7. (Mar. 30, 1999), pp. 3600-3605.

Stable URL:

<http://links.jstor.org/sici?sici=0027-8424%2819990330%2996%3A7%3C3600%3ACSOATT%3E2.0.CO%3B2-Z>

¹⁵ **Plant Ribosome Recycling Factor Homologue Is a Chloroplastic Protein and Is Bactericidal in *Escherichia coli* Carrying Temperature-Sensitive Ribosome Recycling Factor**

Norbert Rolland; Laszlo Janosi; Maryse A. Block; Masahiro Shuda; Emeline Teyssier; Christine Miege; Catherine Cheniclet; Jean-Pierre Carde; Akira Kaji; Jacques Joyard

Proceedings of the National Academy of Sciences of the United States of America, Vol. 96, No. 10. (May 11, 1999), pp. 5464-5469.

Stable URL:

<http://links.jstor.org/sici?sici=0027-8424%2819990511%2996%3A10%3C5464%3APRRFHI%3E2.0.CO%3B2-3>

¹⁶ **Complete Genome Sequence of the Methanogenic Archaeon, *Methanococcus jannaschii***

Carol J. Bult; Owen White; Gary J. Olsen; Lixin Zhou; Robert D. Fleischmann; Granger G. Sutton; Judith A. Blake; Lisa M. FitzGerald; Rebecca A. Clayton; Jeannine D. Gocayne; Anthony R. Kerlavage; Brian A. Dougherty; Jean-Francois Tomb; Mark D. Adams; Claudia I. Reich; Ross Overbeek; Ewen F. Kirkness; Keith G. Weinstock; Joseph M. Merrick; Anna Glodek; John L. Scott; Neil S. M. Geoghagen; Janice F. Weidman; Joyce L. Fuhrmann; Dave Nguyen; Teresa R. Utterback; Jenny M. Kelley; Jeremy D. Peterson; Paul W. Sadow; Michael C. Hanna; Matthew D. Cotton; Kevin M. Roberts; Margaret A. Hurst; Brian P. Kaine; Mark Borodovsky; Hans-Peter Klenk; Claire M. Fraser; Hamilton O. Smith; Carl R. Woese; J. Craig Venter

Science, New Series, Vol. 273, No. 5278. (Aug. 23, 1996), pp. 1058-1073.

Stable URL:

<http://links.jstor.org/sici?sici=0036-8075%2819960823%293%3A273%3A5278%3C1058%3ACGSOTM%3E2.0.CO%3B2-H>

²² **Direct Visualization of A-, P-, and E-Site Transfer RNAs in the *Escherichia coli* Ribosome**

Rajendra K. Agrawal; Pawel Penczek; Robert A. Grassucci; Yanhong Li; ArDean Leith; Knud H. Nierhaus; Joachim Frank

Science, New Series, Vol. 271, No. 5251. (Feb. 16, 1996), pp. 1000-1002.

Stable URL:

<http://links.jstor.org/sici?sici=0036-8075%2819960216%293%3A271%3A5251%3C1000%3ADVOAPA%3E2.0.CO%3B2-0>

NOTE: *The reference numbering from the original has been maintained in this citation list.*

LINKED CITATIONS

- Page 3 of 3 -



²³ **X-Ray Crystal Structures of 70S Ribosome Functional Complexes**

Jamie H. Cate; Marat M. Yusupov; Gulnara Zh. Yusupova; Thomas N. Earnest; Harry F. Noller
Science, New Series, Vol. 285, No. 5436. (Sep. 24, 1999), pp. 2095-2104.

Stable URL:

<http://links.jstor.org/sici?sici=0036-8075%2819990924%293%3A285%3A5436%3C2095%3AXCSO7R%3E2.0.CO%3B2-Y>

³² **Crystal Structure of the Ternary Complex of Phe-tRNA ^{^{Phe}}, EF-Tu, and a GTP Analog**

Poul Nissen; Morten Kjeldgaard; Søren Thirup; Galina Polekhina; Ludmila Reshetnikova; Brian F. C. Clark; Jens Nyborg

Science, New Series, Vol. 270, No. 5241. (Dec. 1, 1995), pp. 1464-1472.

Stable URL:

<http://links.jstor.org/sici?sici=0036-8075%2819951201%293%3A270%3A5241%3C1464%3ACSOTTC%3E2.0.CO%3B2-%23>